

## Intraband transitions in simple metals: Evidence for non-Drude-like near-IR optical properties

H.-G. Boyen, R. Gampp, and P. Oelhafen

*Institut für Physik, Universität Basel, Klingelbergstr. 82, CH-4056 Basel, Switzerland*

B. Heinz and P. Ziemann

*Abteilung Festkörperphysik, Universität Ulm, D-89069 Ulm, Germany*

Ch. Lauinger

*Institut für Physik, TU Chemnitz-Zwickau, D-09107 Chemnitz-Zwickau, Germany*

St. Herminghaus

*Fakultät für Physik, Universität Konstanz, D-78434 Konstanz, Germany*

(Received 2 June 1997)

By combining optical methods with photoelectron spectroscopy on crystalline AuIn<sub>2</sub> films, clear evidence is provided for a non-Drude-like behavior of the intraband contribution to the optical response. The deviation from simple Drude theory is related to a non-free-electron-like density of states, which differs from the standard band shape assumed in the calculation of intraband excitations in ordered simple metals. The close connection between intraband optical and electronic properties is supported by results from amorphous AuIn<sub>2</sub> films, for which a free-electron behavior is consistently observed by both methods. [S0163-1829(97)07335-9]

Among the various properties of crystalline solids, the optical response to incident light is one of the standard phenomena used to characterize materials. Usually, two distinct contributions are considered in the discussion of optical data, arising from momentum-conserving interband transitions and non-momentum-conserving intraband transitions between states separated by the photon energy  $\hbar\omega$ . In simple metals like, e.g., noble metals or noble-metal-based alloys, interband transitions are observed to dominate the optical properties at higher photon energies, whereas in the near-IR domain intraband transitions are known to be responsible for the optical response. For photon energies below the interband absorption edge, the complex dielectric function  $\varepsilon = \varepsilon_1 + i\varepsilon_2$  can be treated within simple Drude theory as

$$\varepsilon_1 = 1 + \varepsilon_\infty - \frac{\omega_p^2 \tau^2}{1 + \omega^2 \tau^2}, \quad (1)$$

$$\varepsilon_2 = \frac{\omega_p^2 \tau}{\omega(1 + \omega^2 \tau^2)}, \quad (2)$$

if a frequency-dependent scattering rate  $\tau^{-1}$ ,

$$\tau^{-1} = \tau_0^{-1} + \beta(\hbar\omega)^2, \quad (3)$$

is assumed. Here,  $\omega_p$  denotes the plasma frequency and  $\varepsilon_\infty$  the core polarizability. Several models have been proposed to account for electron-phonon, electron-electron, and electron-impurity collisions,<sup>1,2</sup> leading to a quadratic dependence of the scattering rate on photon energy as given by Eq. (3). Very often, the above relations have been used to phenomenologically describe the intraband contributions in polycrystalline materials.<sup>3-7</sup> For such systems, however, additional effects may be important. Grain-boundary scattering and surface scattering have been predicted<sup>8,9</sup> to cause deviations from formula (3), yielding an explanation for the ob-

served differences in the optical response between a polycrystalline sample and the corresponding single-crystalline material.

In this contribution we will demonstrate that there exists another important aspect which has not yet been considered in the discussion of intraband excitations in simple metals—the details of the electronic structure. Since all the above theories assume free electrons to be scattered (i.e., a parabolic conduction band), we have investigated both the complex dielectric function and the electronic density of states (DOS) of polycrystalline AuIn<sub>2</sub> in order to clarify the role of the actual band structure. In the following we provide evidence that the description of intraband excitations within the Drude model as proposed for the similar compounds AuAl<sub>2</sub> (Ref. 4) and AuGa<sub>2</sub> (Ref. 6) fails in our case due to inconsistencies in the resulting physical parameters. These inconsistencies are not solely due to scattering effects typical for polycrystalline materials, but rather are a consequence of the non-free-electron-like DOS as determined by x-ray photoelectron spectroscopy (XPS). The close connection between intraband properties and the DOS will be supported by complementary measurements on samples in the amorphous state, where a free-electron behavior is consistently observed in both the optical constants and the electronic structure.

All samples were prepared as thin films ( $D = 30$  nm) evaporated under high-vacuum conditions for the optical and ultra high-vacuum conditions for the photoemission experiments, respectively. For the crystalline alloy, reflection and transmission coefficients were measured under ambient conditions on a two-beam spectrophotometer Cary-5 (Varian) in the photon energy range from 0.4 to 6.7 eV [substrates 0.4–1.0 eV Si(100), 0.9–6.7 eV quartz]. From these data, the optical constants were calculated according to the method described in Ref. 10. To analyze the influence of the oxide overlayer<sup>6</sup> present in these measurements, independent ex-

periments have been performed *in situ* by means of the attenuated-total-reflection (ATR) technique,<sup>11</sup> which is especially useful for the investigation of thin films. Experimentally, different lasers were coupled to the vacuum chamber operating at a finite number of frequencies in the photon energy range between 1.6 and 2.7 eV.

The transformation into the amorphous state was accomplished *in situ* by bombarding a crystalline sample with 350-keV Ar<sup>+</sup> ions at 77 K,<sup>12</sup> followed by the optical characterization using the ATR technique. In this case, optical measurements under ambient conditions could not be performed due to the low crystallization temperature of the amorphous phase ( $T=200$  K). To be able to exclude any influence of implanted Ar atoms or substrate atoms backscattered by the ion bombardment into the film on its optical properties, a crystalline sample was also irradiated with similar fluences at room temperature. In this case, the film maintained its as-prepared crystalline state and no changes of the optical properties could be detected. The photoemission experiments were done on a FISON ESCALAB-210 electron spectrometer, which is equipped with a high-power x-ray source (monochromatized Al  $K\alpha$ ). Depending on the substrate temperature during evaporation (77 K, room temperature), the amorphous or crystalline phase was obtained. In either case, negligible contamination was found by core-level spectroscopy, which, in addition, allowed us to verify the stoichiometry of the alloy. For the characterization of the DOS, the overall instrumental resolution was adjusted to 0.35 eV [full width at half maximum (FWHM)].

In Fig. 1 the real and imaginary parts of the measured dielectric function,  $\epsilon_1$  (a) and  $\epsilon_2$  (b), are presented for crystalline and amorphous AuIn<sub>2</sub>. Concentrating first on the *ex situ* results for the crystalline phase (solid lines), the real part is found to be negative over the whole energy range with a pronounced structure at about 1.8 eV due to strong interband transitions. These can similarly be observed in  $\epsilon_2$ . Here, a broad maximum is visible at 2.2 eV, which, according to band-structure calculations,<sup>13</sup> can be attributed to direct transitions between *sp*-like states along, e.g., the  $\Gamma$ - $X$  direction [see the inset of Fig. 1(b)]. At higher photon energies, additional small structures are observable in  $\epsilon_1$  and  $\epsilon_2$ , indicating that noble-metal *d* states come into play. Thus deviations from a monotonic, Drude-like behavior are evident for energies above 1.5 eV, where interband transitions start to dominate the optical response. This is also confirmed by the *in situ* measurements of the crystalline phase (open symbols), which agree well with the data obtained under ambient conditions. In the disordered state, the optical properties significantly differ from those of the ordered phase. Now, a monotonic behavior can be recognized for energies up to 2.7 eV.

To obtain quantitative results, the intraband contribution to the complex dielectric function has been estimated for both phases by fitting Eqs. (1)–(3) to the experimental results. For the crystalline alloy, the energy range has been restricted to values below 0.5 eV as proposed for AuGa<sub>2</sub> (Ref. 6); for the amorphous alloy, all measured data were used for the numerical analysis. In Table I, the Drude parameters of AuIn<sub>2</sub> are summarized together with a selection of results, reported earlier on similar ordered and disordered systems. Apparently, the free-electron parameters of AuIn<sub>2</sub> appear reasonable in comparison with the other alloys for

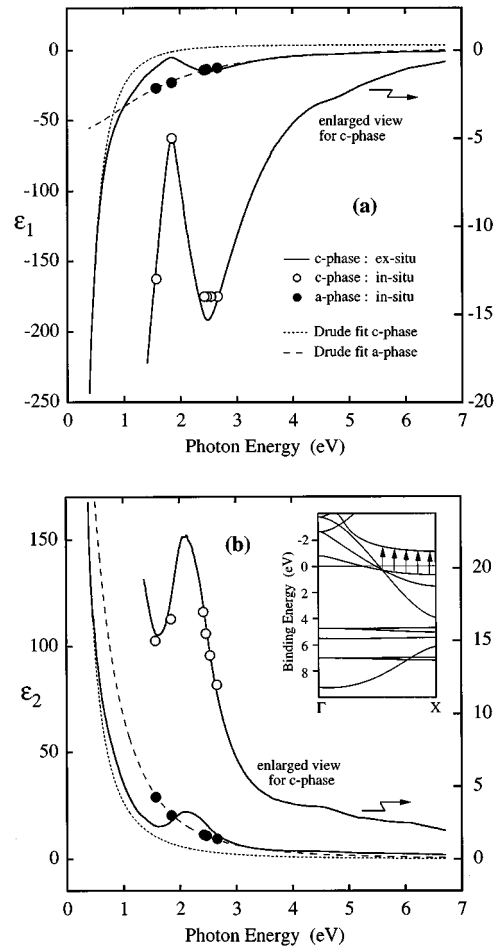


FIG. 1. Real (a) and imaginary (b) parts of the complex dielectric function of AuIn<sub>2</sub> in the ordered as well as the amorphous phase, respectively. The dotted (dashed) line indicates the free-electron contribution in the crystalline (amorphous) state, as determined from the Drude model by means of a least-squares fitting procedure. The inset shows the energy-band structure for the ordered compound along the  $\Gamma$ - $X$  direction (Ref. 13).

both atomic structures. To judge the reliability of this procedure, however, the physical meaning of the parameters has to be examined, too. For the plasmon energy this can be achieved by means of photoemission from inner shells, which is usually accompanied with the excitation of bulk plasmons at wave vectors  $q \approx 0$ , leading to additional structures (plasmon loss peaks) in the corresponding core-level spectra. Photoemission results for the bulk plasmon energies have been added to Table I, showing only a small difference between the ordered and disordered states of AuIn<sub>2</sub>. A similar behavior is known for, e.g., liquid and solid Sn,<sup>14</sup> where the difference in plasmon energy can be attributed to the small density change upon melting. Comparing the Drude parameters  $\hbar\omega_p$  with the experimental results, almost perfect agreement is observed for the amorphous alloy, but a significant discrepancy is visible for the crystalline phase. This already is a strong argument against the applicability of the Drude model for the ordered compound in contrast to the assumption of previous studies,<sup>4,6</sup> though confirming this approach as useful for the amorphous phase.

Since we are interested in correlations between the intraband properties and the actual electronic structure, XPS va-

TABLE I. Drude parameters of crystalline and amorphous AuIn<sub>2</sub>, compared to results from similar systems. In the case of amorphous AuIn<sub>2</sub>, a constant relaxation time ( $\beta=0$ ) was sufficient to fit the experimental data in accordance with earlier studies.

Alloy	$\hbar\omega_p$ (eV)	$\tau_0$ ( $10^{-14}$ sec)	$\beta$ ( $10^{14}$ sec <sup>-1</sup> eV <sup>-2</sup> )	$\epsilon_\infty$	$\hbar\omega_p^{\text{expt}}$ (eV)	Ref.
<i>c</i> -AuIn <sub>2</sub>	7.30	0.44	11.6	2.89	12.6	this work
<i>c</i> -AuGa <sub>2</sub>	4.72	0.602	10.2	2.70		6
<i>c</i> -AuAl <sub>2</sub>	6.368	5.435	3.882	6.30		4
<i>a</i> -Au <sub>33</sub> In <sub>67</sub>	12.1	0.0425		2.37	12.2	this work
<i>a</i> -Au <sub>25</sub> Sn <sub>75</sub>	9.8	0.037				19
<i>a</i> -Au <sub>76</sub> Ge <sub>24</sub>	12.46	0.0285		1.78		20

lence band spectra of both phases are presented in Fig. 2 (solid lines). It is well known<sup>15</sup> that an XPS experiment on a polycrystalline sample provides information about the DOS of the material, since the momentum selection rules are averaged out. No azimuthal dependences of spectra occur like in photoelectron diffraction experiments, where high-quality single-crystalline materials are needed. Thus an XPS spectrum taken from a polycrystalline sample represents the sum of angular-momentum-projected densities of states weighted by the corresponding photoionization cross sections. To get more insight into the distribution of conduction states for polycrystalline AuIn<sub>2</sub>, the corresponding XPS spectrum may be interpreted<sup>15</sup> along the calculated DOS of the single-crystalline phase,<sup>13</sup> broadened to account for lifetime effects and the instrumental resolution (Fig. 2, dotted curve). A close resemblance is observed between both sets of data as

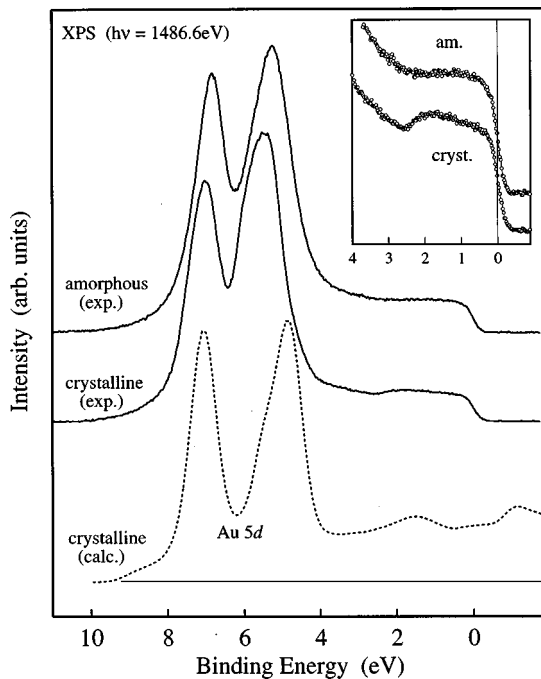


FIG. 2. XPS valence band spectra of AuIn<sub>2</sub> in the polycrystalline and amorphous state (solid lines), compared with DOS results (Ref. 13) for the ordered compound (dotted line). The theoretical curve has been broadened to account for lifetime and instrumental resolution effects. The experimental data, which have been acquired under normal incidence, are corrected for secondary electrons by means of a Shirley type of background (Ref. 21).

far as the general shape is concerned, including the total bandwidth, the Au 5*d*-band features, and the existence of a peak at a binding energy of about 2 eV, which can be attributed to states with pure *sp* symmetry.<sup>13</sup> Our results on the ordered phase are partially supported by earlier investigations,<sup>16</sup> which, due to lower instrumental resolution and poorer statistics, could not resolve the intensity maximum at low binding energy, clearly visible in our data. Since there is good overall agreement between the theoretical and experimental band shapes for the ordered compound, the photoemission results may be considered as a reliable representation of the occupied part of the DOS, which can also be expected for the spectrum of the amorphous phase.

With the results for the crystalline and the amorphous phase, it is straightforward to examine whether or not free electrons are responsible for the optical properties at low photon energies as commonly assumed by theory in calculating the influence of scattering effects in ordered simple metals. This can be achieved by a closer inspection of the DOS at low binding energies, shown enlarged in the inset of Fig. 2. Obviously, a negative slope can be identified for the polycrystalline specimen for energies up to the Fermi level,  $E_F$ , where the instrumental resolution leads to a smearing of the steplike Fermi function. This result is at variance with the assumption of a free-electron- (square-root-) like DOS near the Fermi surface, giving a second experimental argument against the applicability of the Drude model for the ordered phase. For the amorphous sample, however, the absence of the *sp*-band maximum turns out to be the most distinguishing feature between both structures, beside small changes in the Au 5*d*<sub>5/2</sub>-band shape and its position. Additionally, for this sample a plateaulike DOS is observed, extending to binding energies as high as 2.5 eV. This behavior appears to be much closer to a slowly increasing square-root-like DOS as expected for a free-electron model.

Thus a close connection between the electronic structure and the intraband optical properties emerges from the above data, since both the failure of the Drude model for the ordered state as well as its applicability for the disordered phase can consistently be related to the DOS at low binding energies. The failure of the Drude model to describe the near-IR properties of a crystalline metal (or, more generally, of the assumption of free electrons to be scattered) is not too unexpected, since this approach suffers from a considerable conceptual problem: Whereas the interband excitations are generally treated within the framework of band-structure

calculations and electric dipole transitions between single-particle Bloch states,<sup>6,7,17,18</sup> the intraband transitions are attributed to a different class of states (the free electrons), neglecting all selection rules except energy conservation for the excitation process. However, since a band-structure calculation describes all valence electrons present in a given system, intraband transitions must necessarily occur between the same electron states used to calculate the interband part of the dielectric function. Therefore, to arrive at a more consistent description, the intraband transitions should also be treated on the basis of band-structure results, coupling different electronic states by means of scattering matrix elements (describing collisions with other electrons, phonons, grain boundaries, surfaces, impurities, and defects) and dipole selection rules. This point of view is supported by the fact that intraband transitions—like interband transitions—must necessarily change the symmetry of the excited electron in order to account for the angular momentum of the absorbed photon. Depending on the details of the electronic structure, deviations from a simple Drude behavior may occur not only below the interband absorption edge, but within the whole

energy range generally used to investigate the optical properties. Consequently, it remains a questionable procedure to subtract a “Drude background” from the optical constants prior to the discussion of interband excitations as has been done earlier for ordered metals similar to AuIn<sub>2</sub>.

In conclusion, AuIn<sub>2</sub> films have been investigated combining optical methods with x-ray photoemission as well as low-temperature ion bombardment with an *in situ* ATR technique. By analyzing the optical and electronic properties for different atomic structures (polycrystalline, amorphous), a close connection is found between the intraband contribution to the optical response and the details of the electronic structure. This provides clear experimental evidence for the failure of the standard procedure analyzing optical data based on subtracting a “Drude background” and, thus, offers an important new aspect in the discussion of intraband excitations in ordered simple metals.

Financial support by Schweizer Nationalfonds (NF) and Deutsche Forschungsgemeinschaft (DFG) is gratefully acknowledged.

<sup>1</sup>R. T. Beach and R. W. Christy, Phys. Rev. B **16**, 5277 (1977).

<sup>2</sup>J. B. Smith and H. Ehrenreich, Phys. Rev. B **25**, 923 (1982).

<sup>3</sup>Liang-Yao Chen and D. W. Lynch, Phys. Rev. B **36**, 1425 (1987).

<sup>4</sup>Liang-Yao Chen and D. W. Lynch, Phys. Status Solidi B **148**, 387 (1988).

<sup>5</sup>Kwang Joo Kim, Liang-Yao Chen, and D. W. Lynch, Phys. Rev. B **38**, 13 107 (1988).

<sup>6</sup>Kwang Joo Kim, B. N. Harmon, L.-Y. Chen, and D. W. Lynch, Phys. Rev. B **42**, 8813 (1990).

<sup>7</sup>Kwang Joo Kim, B. N. Harmon, and D. W. Lynch, Phys. Rev. B **43**, 1948 (1991).

<sup>8</sup>J. C. Dudek, Thin Solid Films **152**, 411 (1987).

<sup>9</sup>J. C. Dudek, Thin Solid Films **137**, 11 (1986).

<sup>10</sup>E. Elizalde and F. Rueda, Thin Solid Films **122**, 45 (1984).

<sup>11</sup>J. R. Sambles, G. W. Bradbery, and F. Yang, Contemp. Phys. **32**, 173 (1991).

<sup>12</sup>W. Miehle, A. Plewnia, and P. Ziemann, Nucl. Instrum. Methods Phys. Res. B **59/60**, 460 (1991).

<sup>13</sup>Sehun Kim, J. G. Nelson, and R. S. Williams, Phys. Rev. B **31**, 3460 (1985).

<sup>14</sup>G. Indlekofer, Ph.D. thesis, University of Basel, Switzerland, 1987.

<sup>15</sup>S. Hüfner, in *Photoelectron Spectroscopy*, edited by M. Cardona, Springer Series in Solid State Sciences, Vol. 82 (Springer, Berlin, 1995), p. 355.

<sup>16</sup>P. M. v. Attekum, G. K. Wertheim, G. Crecelius, and J. H. Wernick, Phys. Rev. B **22**, 3998 (1980).

<sup>17</sup>Bong-Soo Kim, B. N. Harmon, and D. W. Lynch, Phys. Rev. B **39**, 13 146 (1989).

<sup>18</sup>V. N. Antonov, V. N. Antonov, O. Jepsen, O. K. Andersen, A. Borghesi, C. Bosio, F. Marabelli, A. Piaggi, G. Guizzetti, and F. Nava, Phys. Rev. B **44**, 8437 (1991).

<sup>19</sup>D. Korn and H. Pfeifle, J. Phys. F **9**, 1175 (1979).

<sup>20</sup>M. L. Theye, V. N. Van, and S. Fisson, Philos. Mag. B **47**, 31 (1983).

<sup>21</sup>D. A. Shirley, Phys. Rev. B **5**, 4709 (1972).